

Geology and Petrography of the Ash-Sharqi Granitoid Pluton, Southwestern Yemen

Abdul-Hamid Malek* and Mukhtar A. Nasher

Geology Department, Faculty of Applied Science, Taiz University, Taiz, Yemen

Received January 19, 2023; Accepted September 3, 2023

Abstract

A reconnaissance study of the Ash-Sharqi area displays that this area is covered by Tertiary rift-related volcanic rocks and their associated plutonic rocks with some exposures of Mesozoic sandstones. These volcanic rocks belong to the Yemen Trap Series (YTS) that form the lower part of the Yemen Volcanic Group (YVG), which consists of a part of the Afro-Arabian continental flood basalt province. The plutonic rocks are represented by intrusion composed of granitoid rocks located in the center of the study area, which is the subject of this paper. These granitoid rocks range in composition from granite (G) to quartz-monzonite - quartz-monzodiorite – quartz diorite (QM-QMD-QD) and are composed of plagioclase (An32-46: Andesine), K-feldspars, quartz, hornblende with minor, biotite, opaques, allanite and zircon. Secondary minerals are represented by chlorite, sericite calcite sphene, hematite epidote, and kaolinite. These rocks show variations in their colors (color index 6 to 47 vol. %) and grain sizes, which reflect changes in mineral composition and textures. They have equigranular, porphyritic, rapakivi, and anti-rapakivi textures and contain enclaves of various sizes of basalt and diorite blocks. Xenocrysts of pyroxene and plagioclase are found and detronated during the magma-mingling processes. Finally, these granitoid rocks are subjected to various degrees of hydrothermal alterations, including silicification, argillization, hematitization, chloritization, epidotization, sericitization, carbonation and spheronization.

© 2024 Jordan Journal of Earth and Environmental Sciences. All rights reserved

Keywords: Ash-Sharqi, Granitoid, Monzogranite, Granodiorite, Quartz-monzonite, Enclaves, Alteration, Rapakivi.

1. Introduction

The Cenozoic igneous activity in Yemen is a part of the widespread Afro-Arabian continental flood basalt province, which is related to the continental rifting and formation of the Gulf of Aden and the Red Sea basins (Mohr and Zanettin 1988; Baker, et al. 1996; Ukstins et al. 2002; Nasher, et al. 2020). They are due to Afar-field stress generated by slab-pull in a subduction zone (Menzies et al. 1990; Robertson Group. PLC 1991) and the arrival of Afar plume beneath this region. This continental flood province covers an area of about 600,000 km² (Baker, et al.1996) extending from southwest Ethiopia, through Djibouti, Eritrea, southwest Yemen, northwest of Saudi Arabia, Jordan, and Syria up to Turkey (Al-Malabeh, 1994; Al-Malabeh et al. 2004; El-Hasan and Al-Malabeh 2008; Al Smadi et al. 2018; Sharadqah et al. 2020).

In Yemen, all Cenozoic volcanic rocks and their allied intrusion are termed as Yemen Volcanic Group (YVG) (Menzies et al. 1990; Robertson Group. PLC 1991; Davison et al. 1994; Mattash 1994; Beydone et al. 1998) and are dated from the Late Oligocene to recent times (Mattash 1994; J. A. Baker et al. 1997; Volker et al. 1997; Bosworth, et al. 2005).

The YVG covers an area of about 50,000 km² of the western part of Yemen (Mattash 1994; Beydone et al. 1998) and is divided into older Yemen Trap Series (YTS) (late Oligocene-early Miocene) and younger Yemen Volcanic Series (YVS) (late Miocene-Recent) (Mattash 1994).

Yemen Trap Series (YTS) covers an area of about

42000 km² from which is subtracted about 2000 km² for the granitoid intrusions leaving about 40000 km² of volcanic materials (Beydone et al. 1998).

The granitoid intrusions are exposed essentially in the west border of the Yemen Plateau as Jabal Hufash, Jabal Bura, Jabal Dubes, Jabal Hirsh, Jabal Sabir, Jabal Kabba, and Ash-Sharqi (Figures 1a and b). Some information on the geology, mineralogy, geochemistry, petrogenesis, and tectonic position of the Tertiary granitoid plutons are available in the literature (Al-Kadasi 1988; Youssef, et al. 1992; M. H. Youssef 1993; Kruck and Schaffer 1996; Khanbari 2008; El-Gharbawy 2011; Malek, et al. 2014; Al-Qadhi, A. et al. 2016). Detailed field observations, petrographic inspections and chemical compositions of some Tertiary granitic rocks in Taiz area are given in (Al-Kadasi 1988; Youssef, et al. 1992; Khanbari 2008; El-Gharbawy 2011 a, b). Among these granite intrusions are the Sabir, Ash-Sharqi, and Kabba, which are prominent geomorphological landmarks in the Taiz district (southern Yemeni highlands), at an elevation of 3000 m, 2650 m, and 2350 m above sea level respectively (Figures 1c, d and e).

The previous studies on the Ash-Sharqi area are limited and have focused on the regional geological mapping features (Al-Kadasi 1988; Robertson Group. PLC 1991; Kruck and Schaffer 1996) but this study aims to carry out a detailed investigation of the lithological diversity, geological mapping and later alterations for the granitoid rocks of the study area (Figures 1d and e).

* Corresponding author e-mail: a_malek74@yahoo.com

2. Geologic Setting

The study area lies in southwestern Yemen at latitude $13^{\circ} 27' 39'' - 13^{\circ} 32' 54''$ N and longitude $43^{\circ} 48' 49'' - 43^{\circ} 56' 04''$ E (Figures 1a,b). The field survey indicates that the area consists of sandstone overlain by a thick succession of volcanic rocks (commonly basalt) (Figures 1c, d). The volcanic succession was intruded by Ash-Sharqi pluton and was followed by mafic and felsic dykes. The Ash-Sharqi pluton is one of several Tertiary plutons distributed in the south and west Yemeni highlands. The Jabal Sabir and Jabal Kabba mountains are the most important neighbouring plutons located in the southern Yemeni highlands at an elevation up to 3000 m above sea level. They are the youngest granitoid

plutons that intruded into late Tertiary volcanic rocks which may have originated from material derived from the same magma (Al-Kadasi 1988; El-Gharbawy 2011; Youssef, et al. 1992; Malek, et al. 2014; Al-Qadhi, et al. 2016). Sabir pluton shows diverse topographic features with a peak rising 2980 m above sea level, which stretches in a W-E direction in 9.5 km long and 7 km wide with a total area of around (65 km²). The rocks intrude the volcanic rocks with sharp intrusive contacts and are locally capped by them (Al-Kadasi 1988; Malek, et al. 2014). Kabba pluton forms an oval-shaped body of 4.8 km diameter, which elongated in a NE-SW direction (11.5 km²). It is injected in volcanic sequence and is invaded by basalt and rhyolite dykes (Al-Kadasi, 1988).

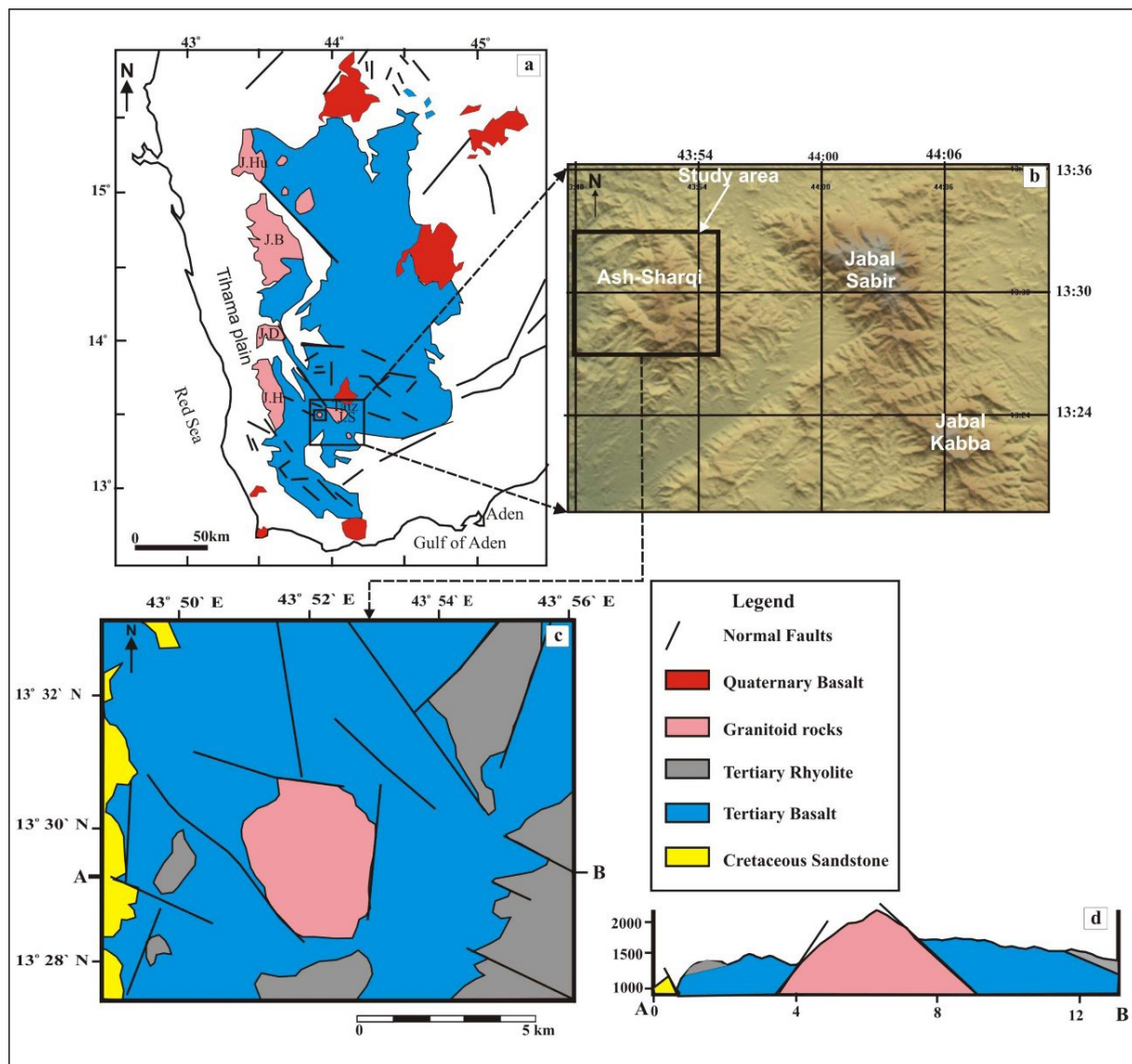


Figure 1. The regional and local position of Tertiary granitic plutons (a) Geological map of western Yemen (modified after (Coleman et al. 1992) displaying the distribution of Cenozoic volcanic and intrusive rocks, (J.Hu) = Jabal Hufash, (J. B.) = Jabal Bura, (J. D) = Jabal Dubes, (J.H) = Jabal Hirsh and (J.S) = Jabal Sabir. (b) DEM of Taiz area showing the location of the study area. (c) Geological map of the Ash-Sharqi area (d) A-B cross section through the mapped area, showing a relationship between rock units and faults.

3. Methods and Scope

This work investigates geological features, which are required for the understanding of a geological map of the Ash-Sharqi area. It includes the description of different rock units with emphasis on granitoid pluton. Besides, studying

field features, geological boundaries, alterations, structures, and sampling of diverse rock types (51 samples) gives reconnaissance geological and mineralogical information of the study area. Field works were carried out along roads, footpaths, and valley channels using the Global Positioning System (GPS) to take accurate positioning and coordinates,

Brunton Compass for measuring data orientation, tap for measuring dimensions, and hammer for sampling. Fresh and altered rock samples were carefully selected for the thin sectioning. The 28 thin sections were studied by using a polarizer microscope. The 16 thin sections were selected for modal analysis by using point counting under a polarizing microscope with an average of 550 counts for each thin section.

4. Results and Discussion

4.1 Field Description

4.1.1 Cretaceous Sandstone

The oldest recognized rocks in the area are clastic sediments that consist of predominantly sandstone, which are correlated with the Tawilah sandstone group, which is exposed in the extreme western part of the mapped area. It is buff to white, fine to medium-grained intercalated with thin beds of shales and conglomerates. The sandstone beds were gently dipping in varying directions causing rupturing by normal faults (Figure 2a).

4.1.2 Volcanic Rock Succession

The volcanic rock succession occurring on most sides of the mapped area, which are mostly basalt in the form of sub-horizontal lava flows, erupted through fissures and intercalated with sporadic cycles of eruption of felsic magma (rhyolite) and pyroclastic rocks. The thickness of this succession is very variable, up to 1500 m in east and south regions (Figure 2b). The basalt flows are generally thick and in some places are thin, grading upward to vesicular and amygdaloidal. The boundaries between basalt flows and felsic or pyroclastic layers are generally sharp, but locally they are gentle with no evidence of erosion traces (Figure 2c). No sediment intercalations have been observed in the volcanic succession. Basaltic flows are commonly aphanitic with subordinate porphyritic containing plagioclase phenocrysts (Figure 2d). Several columnar jointing and entablature columnar jointing and a low amount of vesicles are found in basalt flows (Figure 2e). Some fractures and vesicles are filled with secondary minerals.

The rhyolites are light-colored rocks, aphanitic to porphyritic as phenocrysts of feldspars, impeded in a fine-grained groundmass of feldspar, quartz, and biotite. Pyroclastic rocks, mainly tuff, with subordinate lapilli-tuffs and intercalated tuff-breccia. The tuff units vary in thickness from some centimeters' to a few meters.

The pyroclastic rocks differ in their welding from densely to poorly. The densely welded tuffs are massive and they commonly show highly fractured. The tuff contained either crystal or fragment-rich. The volcanic breccias commonly consist of medium to coarse volcanogenic clasts (usually basaltic clasts) ranging in size from 1 centimeter to nearly 1/2 m diameter with various matrix colors from dark to light grey (Figure 2f). This means that the breccias are spatially and temporally related to the basaltic and rhyolitic eruptions.

4.1.3 Granitoid Rocks

The Ash-Sharqi pluton forms high relief mountains in an oval shape slightly elongated in N-S direction 4 km long and up to 3.4 km wide (11.7 km²) and surrounded from all sides by Tertiary volcanic rocks. The geological boundaries between pluton and volcanic rocks are sharp with cross-cutting relationships characterized by intense post-emplacment alterations and show some deformation features (Figure 3a). The Ash-Sharqi pluton mainly diversifies in colors from light grey rocks to darker types (Figure 3b). The lighter grey rocks are massive, medium to fine-grained with locally coarse-grained. The darker grey rocks occur in the west portion of the granitic pluton medium-grained and equigranular, while finer grained ones occur mainly along the boundaries of the pluton. The alteration zone was produced from hydrothermal alteration and hydration processes that led to the formation of fine-grained quartz and clay minerals. The brecciated contacts and deformation contacts were created from extensive injections of granitic material into a fractured basalt country rock (Figure 3c). The granitoid blocks were locally weathered into spheroidal large blocks (Figure 3d).

4.1.4 Enclaves

Several enclaves of mafic and felsic rocks are seen within the granitoid rocks (Figures 4a and b), which are considered typical features of bimodal magmatism (Tarelow Neto et al 2017). The mafic enclaves are more abundant, dark, rounded to oval-shaped, and range in size from small to large enclaves (a few meters long). Some mafic enclaves have coarser grain sizes, which reflect their deep sources, while the others display finer grain sizes, which may be derived from the surrounding basaltic rocks. Contacts between mafic enclaves and the surrounding granitoid rocks are generally sharp and rarely gradational, with chilling margins characterized by very thin zones (Figure 4a). Mafic enclaves are commonly distributed in the upper part of the granitic pluton and are less common and smaller in the deeper parts that are exposed by erosion. The abundant occurrence of the mafic enclaves in the outer parts of the pluton indicates that this pluton is situated at a relatively shallow depth (El-Gharbawy 2011 a) with incomplete mixing, interaction, and mingling between two types of magmas (Baxter and Feely 2002; Arslan and Aslan 2006; Renna, et al. 2006; Jerram et al. 2011; Perugini and Poli 2012; Ashok et al. 2022; Clemens 2022). In some places, the mafic enclaves have been weathered into reddish-brown rocks. The felsic enclaves are rare, lighter, and coarser in grained equigranular as evidenced by the deeper sources.

4.1.5 Dykes

Several late-stage mafic and felsic dikes crosscut the granitoid pluton. The dykes of mafic composition (basalt) are more abundant, while the felsic dykes (rhyolite) are less common (Figures 5a and b). The dykes are vertical to sub-vertical and differ in thickness from 0.1 to 4 m, with extensions up to several kilometres long. The mafic dykes trend NW-SE, while the felsic dykes take different trends. They are displaying high alteration margins and slight alteration towards their centers.

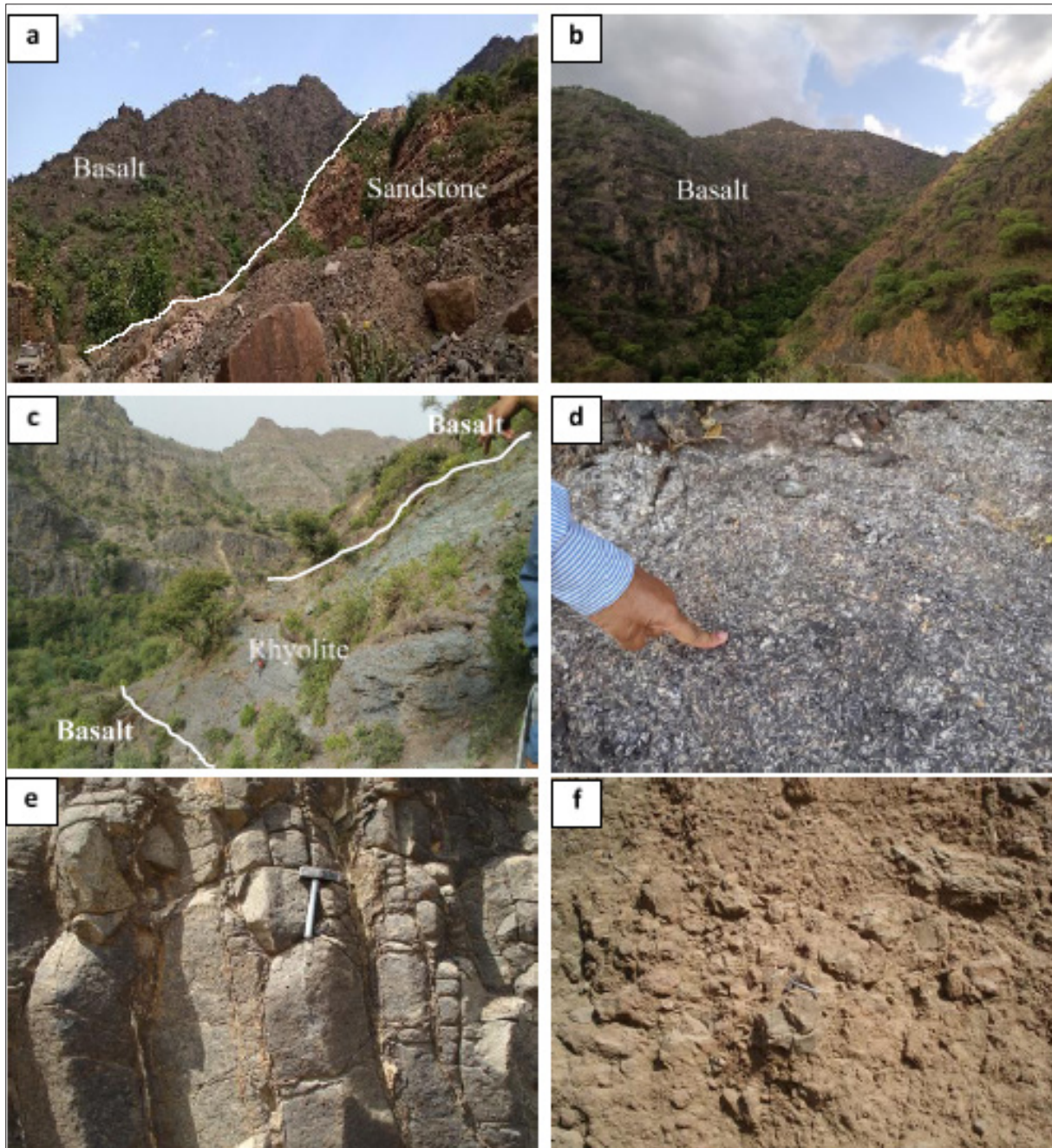


Figure 2. (a). A General view photograph showing the unconformity surface between Tawilah sandstone and Tertiary basalt in the western border of the mapped area. (b) A view showing a huge accumulation of Tertiary basalt at the southern border of granitoid pluton. (c) A view showing light-color rhyolite alternating with dark-colored basalts. (d) Plagioclase phenocrysts display flow structures in basalt. (e) Columnar jointing in basalt (f) Volcani-clastic breccia with basalt fragments in fine-grained tuff matrix

4.1.6 Recent Sediments

Quaternary unconsolidated sediments cover small parts of the study area in the form of poorly sorted clay, silt, sand, gravel, and boulders deposited as alluvial fans at the mouths

of canyons and valleys and as alluvial flood plains bordering ephemeral streams, as landslide deposits and braided-stream sediments filling the drainage channels

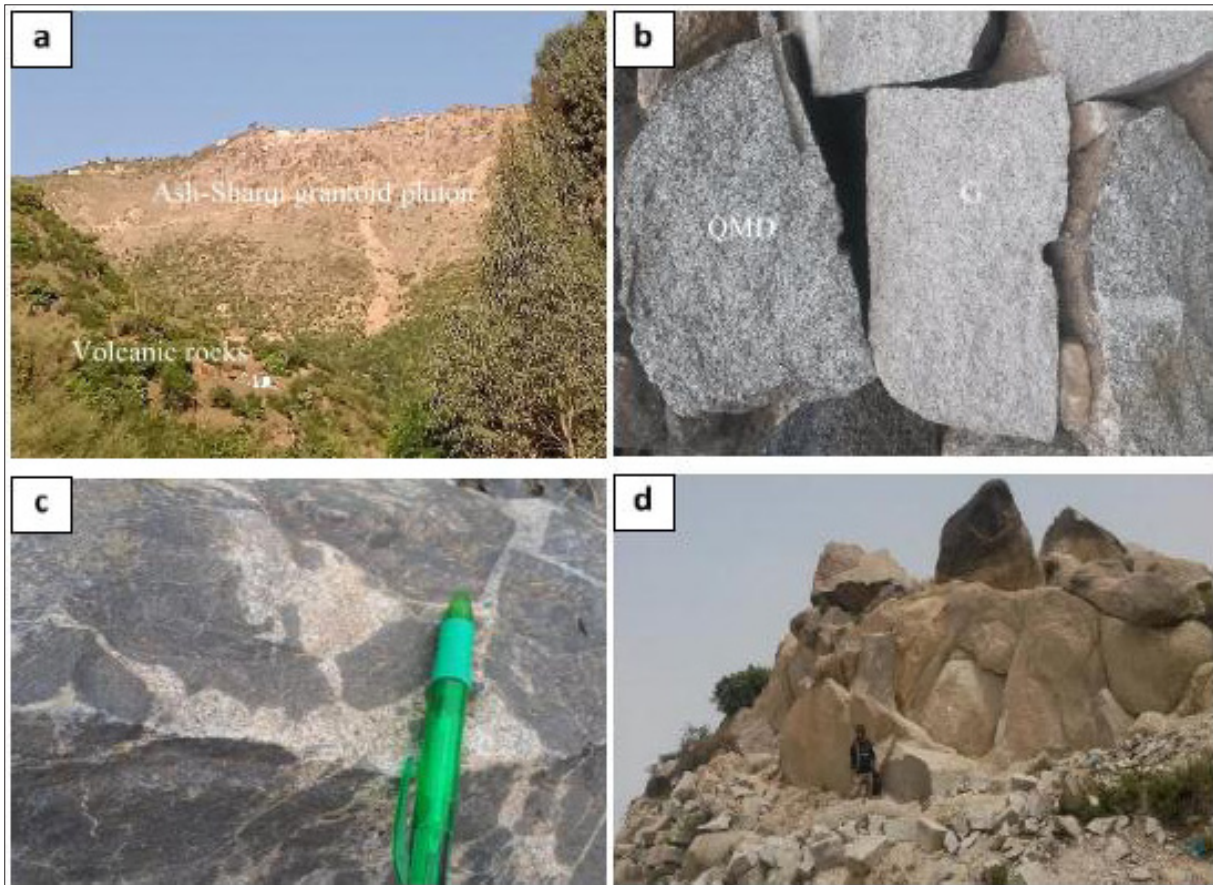


Figure 3. The Field photographs show (a) A general view of the eastern border of granitoid pluton surrounded by volcanic succession. (b) Building stone in the length of 40 cm of granite (GD) (lighter color) and quartz monzodiorite (darker color) (QMD). (c) Injections of granitic melt into fractures at the contact between granitoid pluton and surrounding basalt. (d) Blocky weathering of granitoid rocks with three sets of joints.

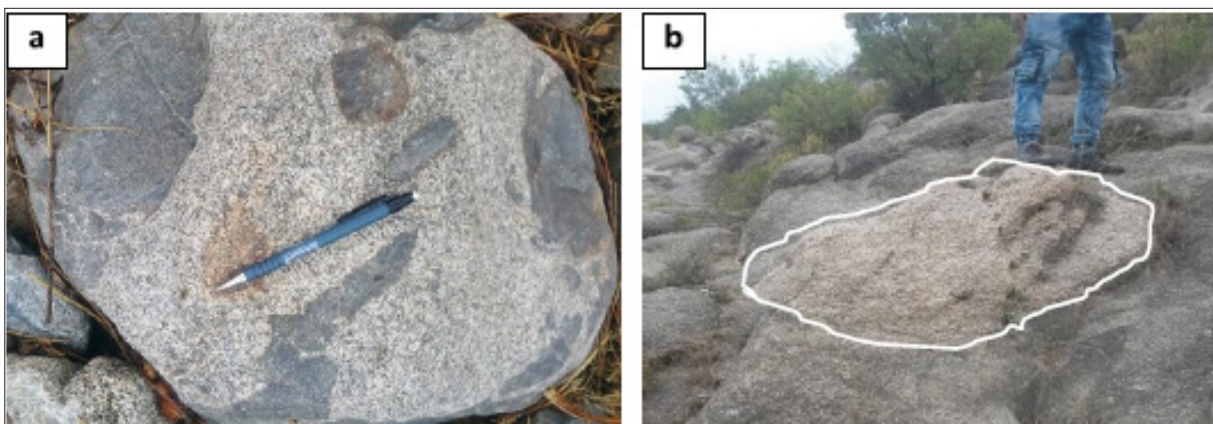


Figure 4. The photographs show (a) mafic enclaves within granitoid pluton, some show chilling margins. (b) Coarse grained felsic enclave within granitoid pluton.



Figure 5. The photographs show (a) The highly altered basalt dyke cutting the granitoid pluton. (c) Rhyolite veins dissecting the granitoid rocks.

4.2 Petrography

Twenty-eight representative samples have been selected from the Ash-Sharqi pluton and its volcanic rocks, dykes, and enclaves' associations for the petrographical studies. The different rock types in the Ash-Sharqi area show analogous and overlapping compositional differences.

The Ash-Sharqi granitoids have been classified based on petrography and the classification scheme of (Streckeisen 1976) into three main groups: 1- Richer in quartz content ($>20\%$) (Granite group G), 2- Moderate content of quartz (5-20%) (quartz monzonite-quartz monzodiorite-quartz diorite (QM-QMD group), and 3- Lower content of quartz ($<5\%$) (Monzodiorite group MD) (Table-1) (Figure 6).

Table 1. Modal composition of selected samples from Ash-Sharqi granitoid rocks (Mineral abbreviations after (Kretz 1983; Siivola and Schmid 2007). The color index (C.I) is calculated as the percentage of dark mafic minerals (M) (Streckeisen, 1976).

Sample	(G)				(QM-QMD)												MD
	As6	As13	As15	As21	As1	As7	As9	As12	As17	As2	As4	As8	As10	As11	As20	As16	
Pl%	25.96	11.21	26.87	23.21	35.63	36.73	32.26	26.32	24.32	48.15	40.95	35.83	40.96	65.52	53.97	69.15	
Kfs%	39.42	53.27	35.82	35.71	20.69	26.53	29.03	46.32	42.34	11.11	9.52	10.83	21.69	10.34	9.52	14.89	
Qtz%	20.19	25.23	23.88	34.82	13.79	13.27	14.52	11.58	14.41	9.26	6.67	6.67	9.64	4.60	9.52	3.19	
Hbl%	6.73	3.74	0.00	0.00	6.90	11.22	8.06	1.05	6.31	3.70	19.05	17.50	9.64	4.60	7.94	0.00	
Bt%	2.88	1.87	4.48	2.68	9.20	4.08	1.61	6.32	5.41	0.00	2.86	3.33	6.02	4.60	1.59	9.57	
Oq%	4.81	2.80	7.46	1.79	4.60	5.10	3.23	5.26	5.41	20.37	12.38	9.17	6.02	5.75	6.35	2.13	
Chl%	-	-	1.49	1.79	2.30	-	6.45	1.05	0.00	-	2.86	5.83	1.20	2.30	-	1.06	
Cal%	-	-	-	0.00	0.00	1.02	0.00	1.05	0.00	-	0.00	0.00	0.00	1.15	-	0.00	
Ep%	-	1.87	-	0.00	5.75	2.04	4.84	1.05	1.80	7.41	5.71	10.83	4.82	1.15	11.11	0.00	
Ttn%					1.15												
Total%	100	100	100	100	100	100	100	100	100	100	100	100	100	100	100	100	
C. I	14	10	13	6	30	22	24	15	19	31	43	47	28	18	27	13	

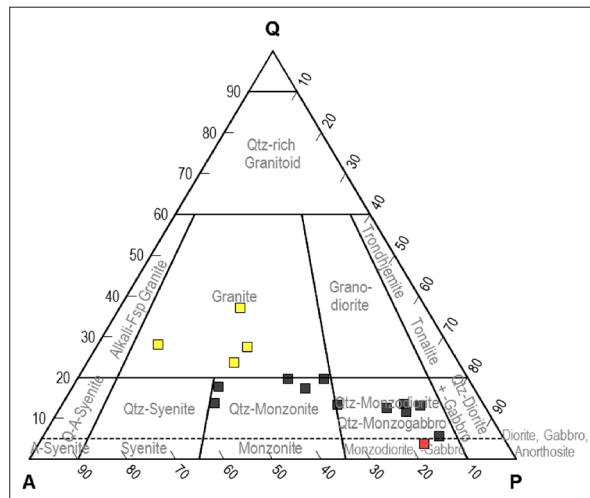


Figure 6. QAP ternary diagram of IUGS classification (Streckeisen 1976) showing modal composition of Ash-Sharqi granitoid rocks. (■) = G, (■) = QM-QMD, (■) = MD.

4.2.1 Granite (G) Group

The G group predominantly crops out in the northern and eastern parts of the study area, varies with its mineral proportions, and shows remarkably hydrothermal alterations. Rocks are generally light (color index (C.I) = 6-14), medium-grained that have a hypidiomorphic granular texture and rare display, porphyritic texture with phenocryst of plagioclase and K-feldspar. The G rocks consist of mainly K-feldspar (36-53%), plagioclase (11-27%), quartz (20-35%),

hornblende (0-7%), biotite (2-4.5%), and magnetite (2-7.5%) as main minerals. Apatite and zircon are common accessory minerals, while sphene, muscovite, sericite, and epidote are secondary minerals (Table-1). K-Feldspars (up to 0.9 mm) are present as anhedral cloudy grains resulted from incipient alteration with some crystals showing myrmekitic texture due to symplectitic intergrowth with the plagioclase. Some K-feldspar grains are corroded by quartz and the others show quartz-feldspar intergrowths on the form graphic or granophyric textures (Figure 7a). Plagioclase (An_{32-38}) exists as subhedral to euhedral plates (up to 0.8 mm), commonly showing albite twinning. The plagioclase crystals have frequently suffered different degrees of sericitization, especially in their inner parts. Quartz (up to 0.4 mm) is present as colorless, anhedral grains, and sometimes exhibits undulatory extinction and found as aggregate pods or form veinlets. Biotite is present as subhedral flakes. It is yellow-brown to brown-green and strongly pleochroic, filling the interspaces between the feldspar grains. Hornblende occurs as anhedral prismatic crystals (up to 0.5 mm), dark green, and strongly pleochroic with Z= dark green, Y= yellow-green, and X= greenish-yellow. It is occasionally replaced by biotite epidote and magnetite as alteration products. Zircon occurs as short prismatic crystals enclosed within plagioclase, quartz, and biotite to form the poikilitic texture (Figure 7b).

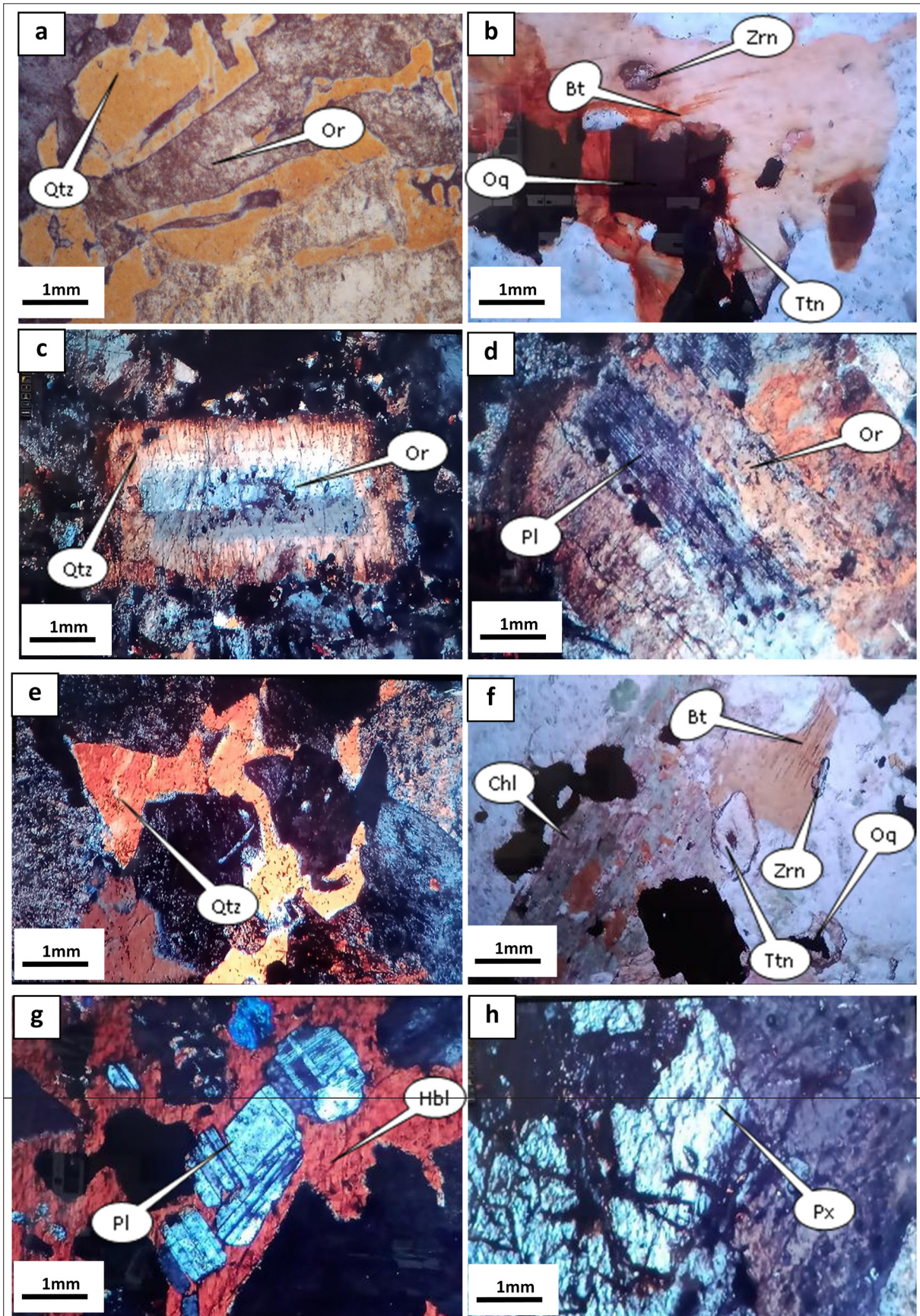


Figure 7. Photomicrographs show (a) Graphic texture produced from intergrowths between K- feldspar (Kfs) and quartz (Qtz). (b) Tiny crystal of zircon (Zrn) enclosed within biotite (Bt) and opaque mineral (Oq) replaced at its margins by titanite (Ttn) (P.L) (c) Phenocrysts of orthoclase (Or) crystal ringed by plagioclase (Pl) forming rapakivi texture. (d) Plagioclase crystal ringed by orthoclase forming anti-rapakivi texture. (e) Quarts surrounding and filling the interstices between the feldspar crystals. (f) Biotite flake replaced by chlorite (Chl), (g) large poikilitic crystal of hornblende (Hbl) enclosing small grains of plagioclase and iron oxide. (h) Part of irregularly resorbed pyroxene (Px) xenocryst display optically continuous with pyroxene in the groundmass.

4.2.2 Quartz Monzonite-Quartz Monzodiorite (QM-QMD) Group

In hand specimens, the QM-QMD are grey to dark grey color (C.I= 15-47), medium to coarse-grained and characterized by an inconspicuous alteration in compared with G.

Microscopically, QM-QMD has allotriomorphic granular texture, composed essentially of plagioclase (37-66%), K-feldspar (10-46%), iron oxides (3-20%), hornblende (1-19%), quartz (5-15%), and biotite (0-9%). Apatite and zircon are accessories. Spene, epidote, chlorite, sericite, and calcite are present as secondary constituents. In the porphyritic types, plagioclase phenocrysts are surrounded by other varieties. In some samples, K-feldspars are mantled by plagioclase, constituting a rapakivi texture, while in the other samples; the anti-rapakivi is also noted (Figures 7c and d) which indicates the mixing between felsic and mafic magmas (Arslan and Aslan 2006).

Plagioclase (An_{34-46}) occurs as anhedral to subhedral, twinned and untwinned plates (up to 0.7 mm), and is sometimes traversed by irregular fractures filled with minute quartz and biotite. Plagioclase both as phenocrysts and in the groundmass are partially altered into sericite and kaolinite, especially at their outer margins and along fractures. It is normally zoned and usually displays albite twinning. K-feldspar (up to 0.5 mm) occurs as anhedral to subhedral plates, showing cross-hatching (microcline) and simple twinning (orthoclase). It is replaced by myrmekite at the contact with adjoining plagioclase. Quartz is present as water-clear anhedral crystals, usually showing wavy extinction. It is found surrounding or filling the interstices between the plagioclase and K-feldspar (Figure 7e). The Biotite mineral occurs as subhedral to anhedral flakes and forms aggregates of small crystals, which are partly replaced by chlorite (Figure 7f). The hornblende is found as irregular crystals, dark green in color, strongly pleochroic with Z= dark green, Y= yellow-green, and X= greenish-yellow, and a maximum extinction angle of 32°. Some hornblende crystals show dark brown color, irregular shape commonly

contain plagioclase and opaque inclusions (Figure 7g). They contain minute iron oxide granules and are partially altered into green chlorite and iron oxide. Iron oxide occurs as euhedral to anhedral grains, usually associated with titanite. Xenocrystic accessory minerals are less common and are represented by pyroxene and plagioclase, which can be inherited from the country rocks during the ascent of granitic magma (Figure 7h).

Chlorite is present as a secondary mineral and is formed at the expense of biotite and hornblende. It displays a wide variation in shapes and colors vary from green to brown color. Allanite occurs as euhedral prismatic zoned crystals of honey brown colour. Zircon is found as short euhedral prismatic crystals enclosed within plagioclase and K-feldspar.

4.2.3 Felsic enclaves (Monzodiorite MD).

In hand specimen, the felsic enclaves are coarse-grained and of light gray color (Figure 8a). Microscopically, the color index (C.I) of felsic enclaves is 13 and has hypidiomorphic granular and intergranular textures. They are composed mainly of plagioclase (69%), K-feldspar (15%), biotite (10%), and quartz (3%). Iron oxides, apatite, and zircon are accessories, while muscovite and sericite are secondary minerals. The modal compositions of felsic enclaves are given in Table 1. Plagioclase (An_{36-40}) exists as subhedral to euhedral plates, up to 10 mm, commonly showing albite twinning and oscillatory zoning (Figure 8b). The plagioclase crystals have frequently suffered different degrees of sericitization, especially in their inner parts. K-feldspar is present mostly as large subhedral to anhedral crystals with irregular boundaries, up to 8mm. It is commonly replaced by myrmekite overgrowths on adjoining plagioclase crystals. Biotite is present as large-sized to medium flakes, up to 9 mm, of greenish-brown color. It is partly altered to green chlorite. Quartz is present as colorless, anhedral grains, up to 2 mm, and sometimes exhibits wavy extinction. Opaque minerals occur as shapeless grains, up to 1 mm across, associated with biotite and sometimes are mantled by spene.

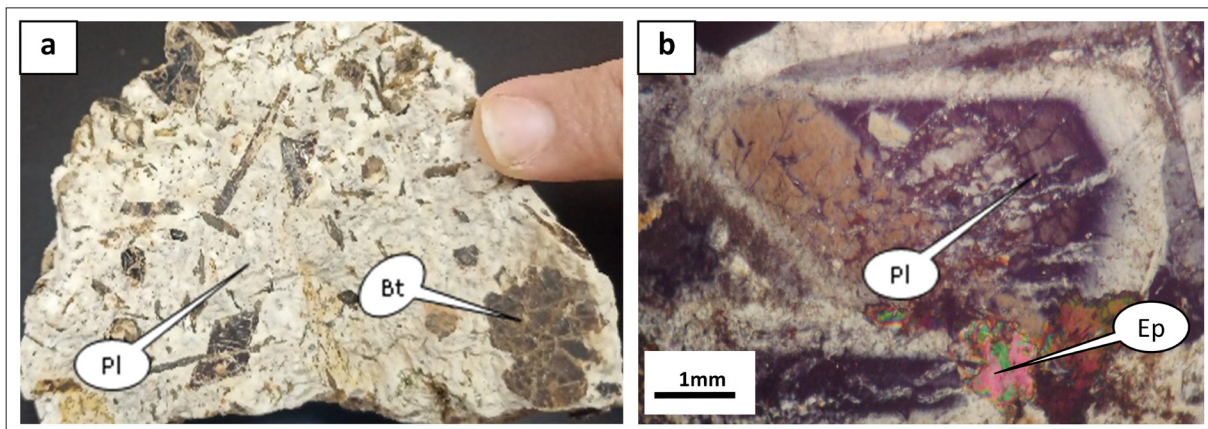


Figure 8. a. A hand-specimen of felsic enclave showing coarse-grained texture consists of plagioclase laths (Pl) and biotite flakes (Bt). (b) A photomicrograph showing euhedrally zoned plagioclase (Pl) partially altered into epidote (Ep).

5. Hydrothermal Alteration

Hydrothermal alteration involves any replacement in the primary mineralogical composition of rock by secondary minerals due to the action of hydrothermal solutions, which take place at temperatures above 50 °C (Galán and Ferrell 2013). Hydrothermal alterations' influence on granitic rocks was studied by several authors. (Ferry 1979; Lee and Parsons 1997; Şener and Gevrek 2000; Boyce et al. 2003; Nishimoto and Yoshida 2010; Jerram et al. 2011; René 2012; Vilalva and Vlach 2014).

The Ash-Sharqi pluton was subjected to hydrothermal alteration owing to the post-magmatic hydrous fluids, which played a major role in the late-stage evolution of the granitic rocks. The hydrothermal alteration is indicated by the extensive silicification, argillization, sericitization, carbonation, chloritization, epidotization, and sphenization processes, which produce several secondary minerals in various manners as replacement products of primary minerals or as patches and as small irregular veinlets cutting the rocks. The degree of alteration varies from very slight to intense, where in very slight alteration; the granitic blocks remain hard to keep their primary minerals and colors, whereas in intense alteration the granitic rocks lose most of their original features and become less coherent and decrease order of strength especially along fractures.

The effect of the alteration on rocks exhibiting cavities and spheroidal features which are commonly noted in the western side of pluton (Figure 9a).

Silicification is produced from reactions with subsequent high-temperature silica-rich solutions ($T = 300-550^{\circ}\text{C}$) (Julia et al. 2014; Ren et al. 2022) or from silica removal associated with chloritization and argillization processes (René 2012). The common silicification processes found as small cavities and Jigsaw veins are filled with chalcedony and quartz. The same filling occurs in the small veinlets traversing the granitic rocks.

Argillization alteration occurs as white to pale yellow zones produced from the influence of hydrothermal solutions on feldspars at low temperatures (50-150 °C) (Julia et al. 2014; Ren et al. 2022), where the feldspars transformed into a mixture of weak and easily deformable rocks consists of clay minerals (Figure 9b). This type of alteration has affected nearly most parts of granitic pluton but in various degrees, where the intense alteration takes place in the south and east sides.

Carbonation alteration is linked with the formation of secondary calcite as a replacement product after Ca-plagioclase and hornblende and as pods and veinlets traversing the other minerals (Figure 9c).

Chloritization alteration occurs under thermal conditions ranging between 150°C and 300°C (Julia et al. 2014; Ren et al. 2022). Two types of chlorite are formed in Ash-Sharqi pluton. Chloritel begins with the creation of very small chlorite spots along the cleavage planes of biotite and hornblende (Figure 9d), which may be associated with the

leaching of iron and the formation of yellow to brown iron staining. Chlorite 2 occurs as veinlets transected plagioclase and K-feldspar.

Sericitization alteration is formed after plagioclase and K-feldspar, where plagioclase shows variable degrees of alteration into sericite especially in their inner parts, while K-feldspar commonly along the outer rim (Figure 9e). This process has almost affected the whole granite body, especially the ones with fissures.

Hematitization alteration process is concentrated in the outer boundaries of the granitic pluton, which gives red to brown color granite, which has been recognized as hematite. In hand samples and under the microscope, hematite is found as veinlets, with a staining effect, which may be attributed to the later stages of oxidation conditions of ferruginous minerals and mafic xenoliths (Figure 9f).

Epidotization found along cleavages and grain boundaries of plagioclase and amphibole (epidote1) (Figure 9g). The epidote is also filled with fissures and intergranular spaces between minerals (epidote 2). Some veins preferentially follow boundaries between plagioclase grains.

Sphenization is a sphene that occurs as single grains or as reaction rim around opaque minerals of Fe-Ti oxides (Figure 9h). That sphenization alteration may be due to the reaction of Fe-Ti oxides with remaining hydrothermal fluids (Imaoka and Nakashima 1982).

6. Structures

The normal faults are the major structures in the area. They separate the granitic pluton and the volcanic succession. In some places, the faults are marked by crushed zones consisting of angular fragments of granite and volcanic rocks (Figure 10a). Extensive alteration of the granite takes place along the faults. The granitic pluton itself was crossed by normal faults and joints, which occur either as open and closed joints (Figure 10b). Sometimes the joints show favored in three directions (two vertical and one horizontal) creating wall parallelepiped joint blocks. The joint spacing decreases for the top of the pluton, and the block size increases towards the base of the pluton. Some fractures are closed and the others are filled by the final stages of solutions. The surfaces of joints are affected by alteration as indicated by the development of clay minerals and are stained on the important spaces within the joint blocks.

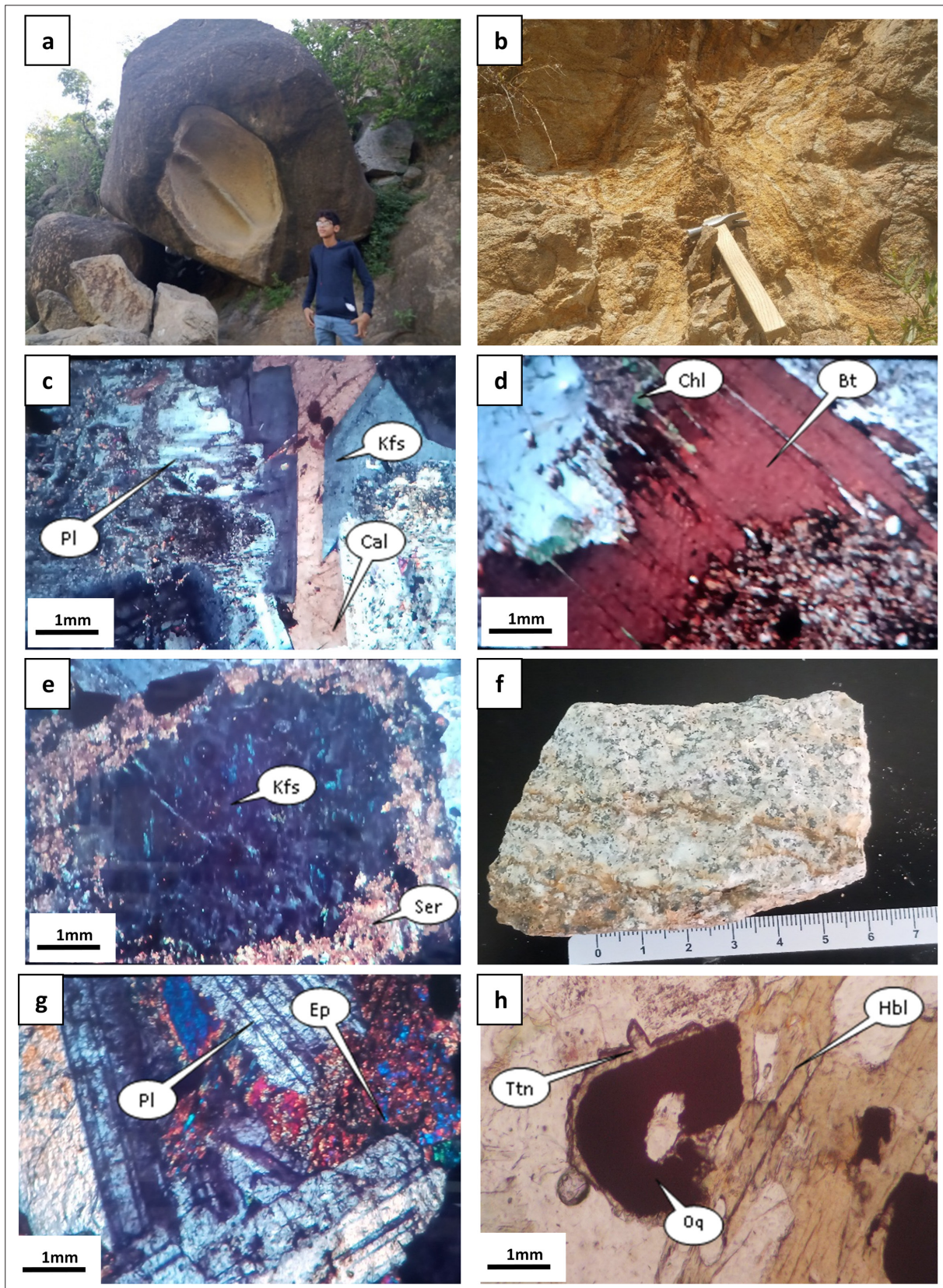


Figure 9. A photograph shows a large cavity within a granite block due to the weathering process. (b) A photograph showing the Argillization alteration zone of the granitoid rocks. (c) A photomicrograph displaying calcite (Cal) vein traversing both plagioclase (Pl) and K-feldspar (Kfs). (d) A photomicrograph showing chlorite (Chl) replacing biotite (Bt). (e) A photomicrograph showing marginally altered K-feldspar (Kfs) into sericite (Ser). (f) A granite hand specimen affected by iron staining along fractures. (g) A photomicrograph showing epidote (Ep) aggregates formed expense plagioclase (Pl). (h) A photomicrograph shows sphene (Titanite) (Ttn) formed expense Fe-Ti oxides (Oq).

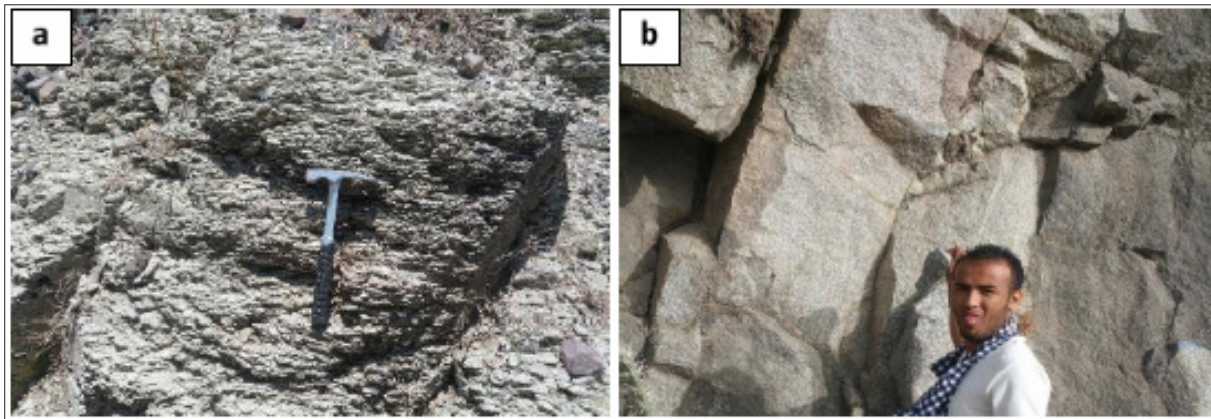


Figure 10. a. A photograph shows crushed zone between granite and basalt. (b) Three sets of joints in granitoid rocks.

7. Conclusions

1- The high magmatic activity of the Western Yemen occurred during the Cenozoic Era and had the following historical evolution:

- (a) Extrusion of huge amounts of basalt flows with minor pyroclastic materials over cretaceous sandstone, followed by extrusion of significant amounts of felsic flows and tuffs with minor pyroclastic.
- (b) Intrusion of a granitoid pluton into earlier volcanic succession.
- (c) Extrusion of basic and felsic flows associated with basic and felsic dykes.
- (d) Faulting and tilting the volcanic succession to their present conditions, where normal faulting took place repeatedly during volcanism, and some movements occurred along the normal faults that occurred after plutonism.

2- Field observations and petrographic investigations of the Ash-Sharqi area recognize five major rock units ordered from bottom to top a- Cretaceous sandstone, b- Tertiary volcanism, c- granitoid pluton, d- mafic and felsic dykes, and e- recent sediments. The present work focuses on granitoid pluton located within the volcanic rock succession.

3- Lithological characteristics and alteration style throughout the Granitoid pluton of Ash-Sharqi area indicate that it is similar to other Tertiary plutons in western Yemen.

4- The Ash-Sharqi pluton is most closely compared to the mainly Sabir pluton. This plutonic suite forms a roughly oval-shaped shape that shows a wider mineralogical variability range in composition from granite to quartz monzonite-quartz monzodiorite-quartz diorite.

5- No clear metasomatic contacts have originated in the area between volcanic succession and granitic pluton.

6- The pre-plutonic mafic, felsic volcanism, post-plutonic mafic, felsic dikes, and magmatic mafic enclaves within the granitic pluton indicate the character of bimodal magmatism.

7- The pluton contained structures such as enclaves and textures such as rapakivi, anti- rapakivi, and resorbed xenocryst indicating the occurrence of magma mixing, interaction, and mingling processes.

8- Hydrothermal alteration and subsequent solutions affecting the granitoid pluton are produced diverse types of alteration processes, including silicification, argillization,

hematitization, chloritization, epidotization, sericitization, carbonation, and spheneization.

9- The study area was affected by various trends of structures on the form: (a) normal faults separate granitoid pluton on surrounding volcanic succession (b) faults and joints crossing granitoid pluton.

References

- Al-Kadasi, M. 1988. "Geology of Gabal Saber Granitic Mass." M.Sc. Thesis, Sana'a University, Yemen.
- Al-Malabeh, A. 1994. "Geochemistry of Two Volcanic Cones from the Intra- continental plateau Basalt of Harra El-Jabban, NE-Jordan." In *Basaltic rocks of Various Tectonic Setting, Special Issue of the Geochemical Journal*. 28: 542-558, Japan.
- Al-Malabeh, A., Al-Fugha, H. and El-Hasan, T. 2004. "Petrology and Geochemistry of Late Precambrian Magmatic Rocks from Southern Jordan". *Neues Jahrbuch fuer Geologie und Palaeontologie*, 233 (3) 333-350.
- Al-Qadhi, A., A, M.R. Janardhana, K.N. Narasimha, and Prakash. 2016. "Field Occurrence and Petrographic Characteristics of Tertiary Volcanic Rocks and Associated Intrusions in and around Taiz City, Yemen." *International Journal of Advanced Earth Science and Engineering* 5 (1): 390–429. <https://doi.org/10.23953/cloud.ijaese.207>.
- Al Smadi, Ali, Ahmad Al-Malabeh, and Sana'a Odat. 2018. "Characterization and origin of Selected Basaltic Outcrops in Harrat Irbid (HI), Northern Jordan." *Jordan Journal of Earth and Environmental Sciences*, 9 (3): 185–96.
- Arslan, M., and Z. Aslan. 2006. "Mineralogy, Petrography and Whole-Rock Geochemistry of the Tertiary Granitic Intrusions in the Eastern Pontides, Turkey." *Journal of Asian Earth Sciences* 27 (2): 177–93. <https://doi.org/10.1016/j.jseas.2005.03.002>.
- Ashok, C., G.H.N.V. Santhosh, S Dash, and J. Ratnakar. 2022. "Magma Mixing and Mingling during Pluton Formation: A Case Study through Field, Petrography and Crystal Size Distribution (CSD) Studies on Sirsilla Granite Pluton, India." *Journal of the Geological Society of India* 98: 815–821. <https://doi.org/https://doi.org/10.1007/s12594-022-2072-4>.
- Baker, J. A., M. A. Menzies, M. F. Thirlwall, and C. G. Macpherson. 1997. "Petrogenesis of Quaternary Intraplate Volcanism, Sana'a, Yemen: Implications for Plume-Lithosphere Interaction and Polybaric Melt Hybridization." *Journal of Petrology* 38 (10): 1359–90. <https://doi.org/10.1093/ptroj/38.10.1359>.
- Baker, Joel, Lawrence Snee, and Martin Menzies. 1996. "A Brief Oligocene Period of Flood Volcanism in Yemen: Implications for the Duration and Rate of Continental Flood Volcanism at the Afro-Arabian Triple Junction." *Earth and Planetary Science Letters* 138 (1–4): 39–55. [https://doi.org/10.1016/0012-821x\(95\)00229-6](https://doi.org/10.1016/0012-821x(95)00229-6).

- Baxter, S., and M. Feely. 2002. "Magma Mixing and Mingling Textures in Granitoids: Examples from the Galway Granite, Connemara, Ireland." *Mineralogy and Petrology* 76 (1–2): 63–74. <https://doi.org/10.1007/s007100200032>.
- Beydone, Z. R., M. A. L. As-Saruri, H. El-Nakhal, I. N Al-Ganad, R. S. Baraba, A. O. Nani, and M. H. Al-Awah. 1998. "International Lexicon of, Republic of Yemen (Second Edition)."
- Bosworth, William, Philippe Huchon, and Ken Mcclay. 2005. "The Red Sea and Gulf of Aden Basins." *Journal of African Earth Sciences* 43: 334–78. <https://doi.org/10.1016/j.jafrearsci.2005.07.020>.
- Boyce, A.J., P. Fulignati, and A. Sbrana. 2003. "Deep Hydrothermal Circulation in a Granite Intrusion beneath Larderello Geothermal Area (Italy): Constraints from Mineralogy FLuid Inclusions and Stable Isotopes." *Journal of Volcanology and Geothermal Research*, 126: 243–62.
- Clemens, J. D. 2022. "Mingling with Minimal Mixing: Mafic-Silicic Magma Interactions in the Oamikaub Ring Complex, Namibia." *Journal of African Earth Sciences* 193: 1–19. <https://doi.org/10.1016/j.jafrearsci.2022.104602>.
- Coleman, Robert G., Susan DeBari, and Zell Peterman. 1992. "A-Type Granite and the Red Sea Opening." *Tectonophysics* 204: 27–40. [https://doi.org/10.1016/0040-1951\(92\)90267-A](https://doi.org/10.1016/0040-1951(92)90267-A).
- Davison, Ian, Mohamed Al-Kadasi, Salah Al-Khribash, Abdul K. Al-Subbary, Joel Baker, Suzanne Blakey, Dan Bosence, et al. 1994. "Geological Evolution of the Southeastern Red Sea Rift Margin, Republic of Yemen." *Geological Society of America Bulletin* 106: 1474–93. [https://doi.org/10.1130/0016-7606\(1994\)106<1474:GEOTSR>2.3.CO;2](https://doi.org/10.1130/0016-7606(1994)106<1474:GEOTSR>2.3.CO;2).
- El-Gharbawy, R. I. 2011 (a). "Petrogenesis of Granitic Rocks of the Jabal Sabir Area, South Taiz City, Yemen Republic." *Chinese Journal of Geochemistry* 30 (2): 193–203. <https://doi.org/10.1007/s11631-011-0501-y>.
- EL-Gharbawy, R. I. 2011 (b). "Contribution to the Geochemistry and Tectonic Setting of the Oligo-Miocene a-Type Granites, South West of the Arabian Shield, Yemen Republic." *Journal of King Abdulaziz University, Earth Sciences*. <https://doi.org/10.4197/Ear.22-2.3>.
- El-Hasan, Tayel, and Ahmad Al-Malabeh. 2008. "Geochemistry, Mineralogy and Petrogenesis of El-Lajjoun Pleistocene Alkali Basalt of Central Jordan." *Jordan Journal of Earth and Environmental Sciences*, 1 (2): 53–62.
- Ferry, J.M. 1979. "Reaction Mechanism, Physical Condition and Mass Transfer during Hydrothermal Alteration of Mica and Feldspar in Granitic Rocks from South-Central Maine, USA." *Contribution to Mineralogy and Petrology* 68: 125–139.
- Galán, E., and R. E. Ferrell. 2013. "Genesis of Clay Minerals." In *Developments in Clay Science*, 5A:83–126. <https://doi.org/10.1016/B978-0-08-098258-8.00003-1>.
- Imaoka, Teruyoshi, and Kazuo Nakashima. 1982. "Iron-Titanium Oxide Minerals of Cretaceous to Paleogene Volcanic Rocks in Western Chugoku District, Southwest Japan Special Reference to Manganese Content of Ilmenites." *J. Japan. Assoc. Min. Petr. Econ. Geol.*, 235–55.
- Jerram, Dougal, and Nick Petford. 2011. *The Field Description of Igneous Rocks. The Geological Field Guide Series (Second Edition)*. Wiley-Blackwell, A John Wiley and Sons, Ltd., Publication. <https://doi.org/10.1017/CBO9781107415324.004>.
- Julia, F, L Vladimir, R Sergey, and Z David. 2014. "Effects of Hydrothermal Alterations on Physical and Mechanical Properties of Rocks in the Kuril–Kamchatka Island Arc." *Engineering Geology* 183: 80–95. <https://doi.org/https://doi.org/10.1016/j.enggeo.2014.10.011>.
- Khanbari, Khaled. 2008. "Study of Structures and Tectonic Evolution of Yemen Tertiary Granites, by Using Remote Sensing Technique." *J. of Remote Sensing* 21: 63–72.
- Kretz, R. 1983. "Symbols for Rock-Forming Minerals." *American Mineralogist* 68 (1–2): 277–79.
- Kruck, W., and U. Schaffer. 1996. "Geological Map of the Republic of Yemen, Sheet Taiz, Scale 1:250,000." Fed. Inst. Geosci. Nat. Res., Hanover.
- Lee, Martin R., and Ian Parsons. 1997. "Dislocation Formation and Albitization in Alkali Feldspars from the Shap Granite." *American Mineralogist* 82 (5–6): 557–70. <https://doi.org/10.2138/am-1997-5-616>.
- Malek, A-H., MR. Janardhana, and A. A. Al-Qadhi. 2014. "Cenozoic Eruptive Stratigraphy and Structure in Taiz Area of Yemen." *Earth Sciences* 3 (3): 85–96. <https://doi.org/10.11648/j.earth.20140303.13>.
- Mattash, M. A. 1994. "Study of the Cenozoic Volcanic Rocks and Their Associated Intrusive Rock in Yemen in Relation to Rift Development." PhD thesis, Hungarian Academy of Sciences and Eotvos L. University., Budapest.
- Menzies, Martin, Dan Bosence, Hamed A. El-Nakha, Salah Al-Khribash, Mohamed A. Al-Kadasi, and Abdulkarim Al Subbary. 1990. "Lithospheric Extension and the Opening of the Red Sea: Sediment-basalt Relationships in Yemen." *Terra Nova*. <https://doi.org/10.1111/j.1365-3121.1990.tb00086.x>.
- Mohr, P, and B Zanettin. 19888. "The Ethiopian Flood Basalt Province." In *Continental Flood Basalts.*, edited by J. D. Macdougall, 63–110. Dordrecht: Kluwer Academic.
- Nasher, Mukhtar A., Mohamed A. Mattash, and Murad A. Ali. 2020. "Geochemistry and Petrogenesis of High-MgO Ultramafic Tertiary Volcanic Rocks from Bagah Area, NW Ad Dhala Province, Yemen." *Arabian Journal of Geosciences* 340: 1–19. <https://doi.org/10.1007/s12517-020-05331-9>.
- Nishimotoa, S, and H Yoshida. 2010. "Hydrothermal Alteration of Deep Fractured Granite: Effects of Dissolution and Precipitation." *Lithos* 115: 153–162. <https://doi.org/doi:10.1016/j.lithos.2009.11.015>Contents.
- Perugini, D., and G. Poli. 2012. "The Mixing of Magmas in Plutonic and Volcanic Environments: Analogies and Differences." *Lithos* 153: 261–77. <https://doi.org/10.1016/j.lithos.2012.02.002>.
- Ren, Minghao, Wei Wang, Zhiquan Huang, Shanggao Li, Qi Wu, Huaichang Yu, and Guangxiang Yuan. 2022. "Effect of Alteration on the Geochemistry and Mechanical Properties of Granite from Pingjiang, Hunan Province, China." *Environmental Earth Sciences* 60: 1–15. <https://doi.org/10.1007/s12665-022-10197-z>.
- René, Miloš. 2012. "Distribution and Origin of Clay Minerals During Hydrothermal Alteration of Ore Deposits." In *Clay Minerals in Nature - Their Characterization, Modification and Application*, edited by Valášková M. and Martynkova S, 81–100. InTech. <https://doi.org/10.5772/48312>.
- Renna, Maria Rosaria, Riccardo Tribuzio, and Massimo Tiepolo. 2006. "Interaction between Basic and Acid Magmas during the Latest Stages of the Post-Collisional Variscan Evolution: Clues from the Gabbro-Granite Association of Ota (Corsica-Sardinia Batholith)." *Lithos* 90 (1–2): 92–110. <https://doi.org/10.1016/j.lithos.2006.02.003>.
- Robertson Group. PLC. 1991. "Geological Map of the Yemen Republic (Taizz) at a 1:250 000 Scale." Sheet No. 13 G.
- Şener, Mehmet, and Ali Ihsan Gevrek. 2000. "Distribution and Significance of Hydrothermal Alteration Minerals in the Tuzla Hydrothermal System, Canakkale, Turkey." *Journal of Volcanology and Geothermal Research* 96 (3–4): 215–28. [https://doi.org/10.1016/S0377-0273\(99\)00152-3](https://doi.org/10.1016/S0377-0273(99)00152-3).
- Sharadqah, S, R A Al Dwairi, M Amaireh, H Nawafleh, O Khashman, A E Al-Rawajfeh and S M Perez 2020. "Geotechnical Evaluation of South Jordan Basaltic Rocks for Engineering Uses" *Jordan Journal of Earth and Environmental Sciences*, 11: 253–59.
- Siivola, J, and R Schmid. 2007. "List of Mineral Abbreviations." IUGS Subcommittee on the Systematics of Metamorphic Rocks, 1–14.

Streckeisen, A. 1976. "To Each Plutonic Rock Its Proper Name." *Earth Science Reviews* 13: 1:33.

Tarelou Neto, J., Pierosan, R., Barros, M. A. de S. A., Chemale, F., and Santos, F. S. 2017. "Magmatic microgranular enclaves of the northeast of Mato Grosso, Brazil, SE Amazonian Craton: Insights into the magmatism of the Uatumã Supergroup on the basis of field and petrological data." *Journal of South American Earth Sciences*, 78, 61–80. <https://doi.org/10.1016/j.jsames.2017.06.004>

Ukstins, Ingrid A, Paul R Renne, Ellen Wolfenden, Joel Baker, Dereje Ayalew, and Martin Menzies. 2002. "Matching Conjugate Volcanic Rifted Margins: Ar / Ar Chrono-Stratigraphy of Pre- and Syn-Rift Bimodal Flood Volcanism in Ethiopia and Yemen." *Earth and Planetary Science Letters* 198: 289–306. [https://doi.org/10.1016/S0012-821X\(02\)00525-3](https://doi.org/10.1016/S0012-821X(02)00525-3).

Vilalva, Frederico Castro Jobim, and Silvio R.F. Vlach. 2014. "Geology, Petrography and Geochemistry of the A-Type Granites from the Morro Redondo Complex (PR-SC), Southern Brazil, Graciosa Province." *Anais Da Academia Brasileira de Ciencias* 86 (1): 85–116. <https://doi.org/10.1590/0001-37652014108312>.

Volker, Frank, Rainer Altherr, Klaus-peter Peter Jochum, and Malcolm T. McCulloch. 1997. "Quaternary Volcanic Activity of the Southern Red Sea : New Data and Assessment of Models on Magma Sources and Afar Plume-Lithosphere Interaction." *Tectonophysics* 278: 15–29. [https://doi.org/10.1016/S0040-1951\(97\)00092-9](https://doi.org/10.1016/S0040-1951(97)00092-9).

Youssef, M. H. 1993. "Tectonic Setting of Some Miocene Granite Intrusions, in Relations to the Aden and Red Sea Rifts, Southwestern Border of the Yemen Plateau." *Geol. Soc. Egypt., Spec. Publ.* 1: 445–59.

Youssef, M, H El-Shatoury, and M Al-Kadasi. 1992. "Geology of Gabal Sabir Granitic Mass, Taizz, Yemen Republic." In *Geology of the Arab World*, 433–447. Cairo: Cairo University.